RODNEY LOUDON

The quantum theory of light

SECOND EDITION

CLARENDON PRESS · OXFORD

3. Fluctuation properties of chaotic light

THE various line-broadening mechanisms described in the previous chapter produce the same lineshapes in both the absorption and emission spectra associated with a given atomic transition. In the present chapter we consider the characteristics of the emitted light generated by radiative transitions of excited atoms. The characteristics can in principle be measured by two different kinds of experiment. Ordinary spectroscopy measures the frequency distribution of the light and thus provides, via the theory outlined in Chapter 2, information on the nature and strengths of the line-broadening processes in the source.

Our main concern in the present chapter is with the second kind of experiment, which measures the time dependence of the amplitude or intensity of the light beam. It is shown that the line-broadening processes in the source also cause the electric field and intensity of the beam to fluctuate around their mean values on a time-scale inversely proportional to the frequency breadth of the light. These temporal fluctuations and the frequency spread are manifestations of the same physical properties of the radiating atoms that constitute the light source, but both aspects are needed to interpret the complete range of optical experiments.

It is important to distinguish between two types of light source. The common spectroscopic source is the gas discharge lamp, where the different atoms are excited by an electrical discharge and emit their radiation independently of one another. The shape of an emission line is determined by the statistical spread in atomic velocities and the random occurrence of collisions. A conventional light source of this kind is called a chaotic source. The thermal cavity and the filament lamp are other examples of chaotic source. The light beams from any variety of chaotic source have a similar statistical description; only the parameters of the statistical distribution vary from one chaotic light beam to another.

The second type of light source is the laser, and this has quite different statistical properties. The properties of laser light are mentioned only briefly in the present chapter, a detailed discussion being deferred until Chapter 7.

The calculations that follow use a classical description of the light beam. The classical model is useful not only for a physical appreciation of the nature

of the fluctuation effects, but also, as is shown in Chapter 6, the classical and quantum theories yield identical predictions for chaotic light. For other kinds of light, where the two theories may differ, the significance of the quantum predictions is more clearly discerned against the background of the corresponding classical theory.

3.1. Spectrum of a fluctuating light beam

Consider an experiment in which a beam of light passes a fixed observation point where the time dependence of its electric field is measured. Much of the present chapter is concerned with the way in which the properties of the light source determine the fluctuation properties of the beam electric field and intensity.

The frequency spectrum of the light at the observation point is determined by the Fourier components of the electric field, defined by

$$E(\omega) = (1/2\pi) \int_{-\infty}^{\infty} E(t)\exp(\mathrm{i}\omega t)\,\mathrm{d}t. \tag{3.1}$$

The cycle-averaged intensity of the light of frequency ω is proportional to

$$\begin{aligned} |E(\omega)|^2 &= (1/4\pi^2) \int_{-\infty}^{\infty}\int_{-\infty}^{\infty} E^*(t)E(t')\exp\{\mathrm{i}\omega(t'-t)\}\,\mathrm{d}t\,\mathrm{d}t' \\ &= (1/4\pi^2) \int_{-\infty}^{\infty}\int_{-\infty}^{\infty} E^*(t)E(t+\tau)\exp(\mathrm{i}\omega\tau)\,\mathrm{d}t\,\mathrm{d}\tau, \end{aligned} \tag{3.2}$$

where

$$\tau = t'-t. \tag{3.3}$$

It is shown in §3.4 that some kinds of optical interference experiment essentially perform the integral over t that appears on the right-hand side of eqn (3.2). The period covered by the integration in a practical experiment is of course never infinite, and we replace the range of the t integration by a large but finite time T. The first-order electric-field correlation function is then defined to be

$$\langle E^*(t)E(t+\tau)\rangle = \frac{1}{T}\int_T E^*(t)E(t+\tau)\,\mathrm{d}t. \tag{3.4}$$

The correlation function describes the way in which the value of the electric field at time t affects the probabilities of its various possible values at a later time $t+\tau$.

The nature of the correlation function will become clear when examples are treated in later sections. Its form is determined by the kind of fluctuations produced by the light source. If the statistical properties of the source are *stationary*, that is the influences that govern the fluctuation statistics do not change with time, then the average in (3.4) does not depend on the particular starting time of the period T provided that T is long compared to the characteristic time scale of the fluctuations. The time averaging in eqn (3.4) can then sample all the electric-field values allowed by the statistical properties of the source with their appropriate relative probabilities, and the result is independent of the magnitude of T. Thus, although the experimental determination of the correlation function is made by a *time* averaging as on the right of eqn (3.4), the function is calculated by a *statistical* average over all values of the field at times t and $t+\tau$. The result does not of course depend on the time t, and the correlation is a function only of the time delay τ between the two field values. The averaging procedure accords with the ergodic theorem mentioned in §1.4.

The intensity (3.2) at frequency ω now becomes

$$|E(\omega)|^2 = (T/4\pi^2)\int_{-\infty}^{\infty}\langle E^*(t)E(t+\tau)\rangle\exp(\mathrm{i}\omega\tau)\,\mathrm{d}\tau. \tag{3.5}$$

This function provides the frequency-dependent spectrum of the light as measured by ordinary spectroscopy. It is convenient to express the spectrum in a normalized form as was done in Chapter 2. The integrated intensity given by eqn (3.5) is

$$\int_{-\infty}^{\infty}|E(\omega)|^2\,\mathrm{d}\omega = (T/2\pi)\langle E^*(t)E(t)\rangle, \tag{3.6}$$

where eqn (2.64) has been used. The normalized spectral distribution function is defined to be

$$F(\omega) = |E(\omega)|^2\Big/\int_{-\infty}^{\infty}|E(\omega)|^2\,\mathrm{d}\omega = (1/2\pi)\int_{-\infty}^{\infty}g^{(1)}(\tau)\exp(\mathrm{i}\omega\tau)\,\mathrm{d}\tau, \tag{3.7}$$

where we have introduced the normalized first-order correlation function

$$g^{(1)}(\tau) = \frac{\langle E^*(t)E(t+\tau)\rangle}{\langle E^*(t)E(t)\rangle}. \tag{3.8}$$

This quantity is called the *degree of first-order temporal coherence* of the light.

The connection (3.7) between the spectrum of the light and its first-order correlation function is a form of the Wiener-Khintchine theorem. It gives the formal relation between the results of spectroscopic experiments and the results of measurements of the time-dependent fluctuation properties of light. The relation can be cast into a form that involves only integration over positive τ and is sometimes more useful. Thus if τ is replaced by $-\tau$ in the integration over negative τ,

$$F(\omega) = (1/2\pi)\int_0^{\infty}g^{(1)}(\tau)\exp(\mathrm{i}\omega\tau)\,\mathrm{d}\tau + (1/2\pi)\int_0^{\infty}g^{(1)}(-\tau)\exp(-\mathrm{i}\omega\tau)\,\mathrm{d}\tau. \tag{3.9}$$

It is however clear from the definition (3.4) that the correlation function depends only on the relative times of the two field measurements, and hence

$$g^{(1)}(-\tau) = \frac{\langle E^*(t)E(t-\tau)\rangle}{\langle E^*(t)E(t)\rangle} = \frac{\langle E^*(t+\tau)E(t)\rangle}{\langle E^*(t)E(t)\rangle} = g^{(1)}(\tau)^*. \tag{3.10}$$

Thus eqn (3.9) becomes

$$F(\omega) = (1/\pi)\mathrm{Re}\int_0^{\infty}g^{(1)}(\tau)\exp(\mathrm{i}\omega\tau)\,\mathrm{d}\tau \tag{3.11}$$

and only the degree of first-order coherence at positive τ is needed to compute the spectrum. The degree of coherence at negative τ can in any case be found from the symmetry property (3.10).

3.2. Model of a collision-broadened light source

The general theory of fluctuations is easily applied to the light generated by a source in which collision broadening predominates. We ignore radiative and Doppler broadening, and we suppose that the collisions are of the elastic phase-interruption variety that does not change the atomic state.

Consider a particular excited atom radiating light of frequency ω_0. One can envisage a wave train of electromagnetic radiation steadily emanating from the atom until it suffers a collision. During a collision, the energy levels of the radiating atom are shifted by the forces of interaction between the two colliding atoms. Thus the radiated wave train is interrupted for the duration of the collision. When the wave of frequency ω_0 is resumed after the collision, its characteristics are identical to those that it had prior to the collision, except that the phase of the wave is unrelated to the phase before the collision.

If the duration of the collision is sufficiently brief, it is possible to ignore any radiation emitted during the collision while the frequency is shifted from ω_0. The collision-broadening effect can then be adequately represented by a model

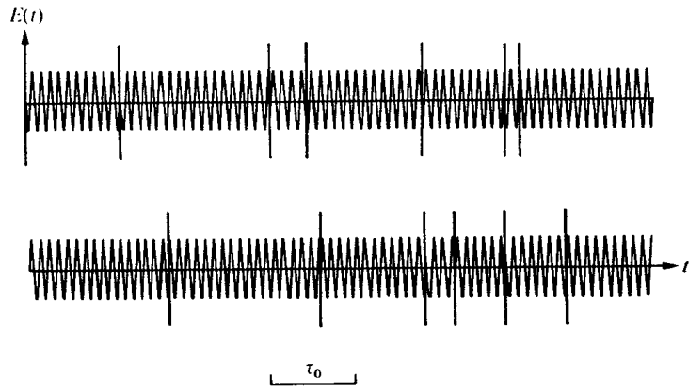

FIG. 3.1. The electric-field amplitude of the wave train radiated by a single atom. The vertical lines represent collisions, separated by periods of free flight with a mean τ_0 of the magnitude indicated. The quantity $\omega_0\tau_0$ is chosen unrealistically small in order to show the random phase changes caused by the collisions.

in which each excited atom always radiates at frequency ω_0, but with random changes in the phase of the radiated wave each time a collision occurs. The apparent spread in the emitted frequencies arises because the wave is chopped up into finite sections whose Fourier decompositions include frequencies other than ω_0.

The wave train radiated by a single atom is illustrated schematically in Fig. 3.1, which shows the variation of the electric field amplitude $E(t)$ at a fixed observation point as a function of time. The occurrence of a collision is represented by a vertical line accompanied by a random change in the phase of the wave. The periods of free flight in the figure are chosen in accordance with the probability distribution (2.131). The variation of the phase of the wave train with time is shown in Fig. 3.2. In order to make Fig. 3.1 easy to draw, the quantity $\omega_0\tau_0$ is given the small value of 60. With the typical value of the collision time given in eqn (2.141) and the visible light frequency given in eqn (1.65), we have

$$\omega_0\tau_0 \approx 9\times 10^4. \tag{3.12}$$

For these values, the wave train radiated by an atom undergoes on average about 15 000 periods of oscillation between successive collisions.

The field amplitude of the wave illustrated in Figs. 3.1 and 3.2 can be written in complex form as

$$E(t) = E_0\exp\{-\mathrm{i}\omega_0 t+\mathrm{i}\phi(t)\}. \tag{3.13}$$

As shown in Fig. 3.2, the phase $\phi(t)$ remains constant during periods of free flight but changes abruptly each time a collision occurs. The amplitude E_0 and

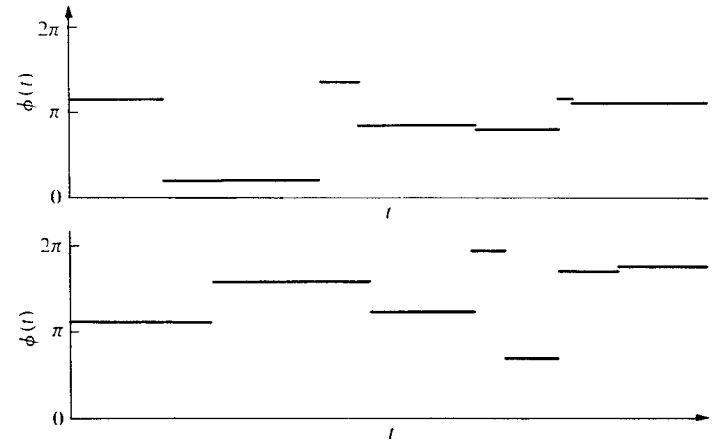

FIG. 3.2. Time dependence of the phase angle of the wave train illustrated in Fig. 3.1.

frequency ω_0 are the same for any period. The total wave emitted by the collision-broadened source is represented by a sum of terms like eqn (3.13), one for each radiating atom. If there is a large number ν of such atoms, the total electric field amplitude is

$$\begin{aligned} E(t) &= E_1(t)+E_2(t)+\ldots+E_\nu(t) \\ &= E_0\exp(-\mathrm{i}\omega_0 t)\{\exp(\mathrm{i}\phi_1(t))+\exp(\mathrm{i}\phi_2(t))+\ldots+\exp(\mathrm{i}\phi_\nu(t))\} \\ &= E_0\exp(-\mathrm{i}\omega_0 t)\alpha(t)\exp(\mathrm{i}\varphi(t)), \end{aligned} \tag{3.14}$$

where every atom has been assigned the same amplitude E_0 and frequency ω_0, but the phases for the different atoms are completely unrelated. It is assumed for simplicity that the observed light has a fixed polarization so that the electric fields can be added algebraically.

The formal summation of the phase factors carried out in the final line of eqn (3.14) is illustrated in Fig. 3.3. Since the phase angles $\phi_1, \phi_2, \ldots, \phi_\nu$ each have different random variations similar to that shown in Fig. 3.2, the amplitude $\alpha(t)$ and phase $\varphi(t)$ are different at different instants of time. The real electric field obtained from eqn (3.14) consists of a carrier wave of frequency ω_0 subjected to random amplitude and phase modulation. The Fourier decomposition of the modulated wave contains frequencies spread about ω_0 in a manner governed by the collision-broadened lineshape.

It is not possible in practice to resolve the oscillations in $E(t)$ that occur at the frequency of the carrier wave. A good experimental resolving time is of order 10^{-9} s, six orders of magnitude too long to detect oscillations at the

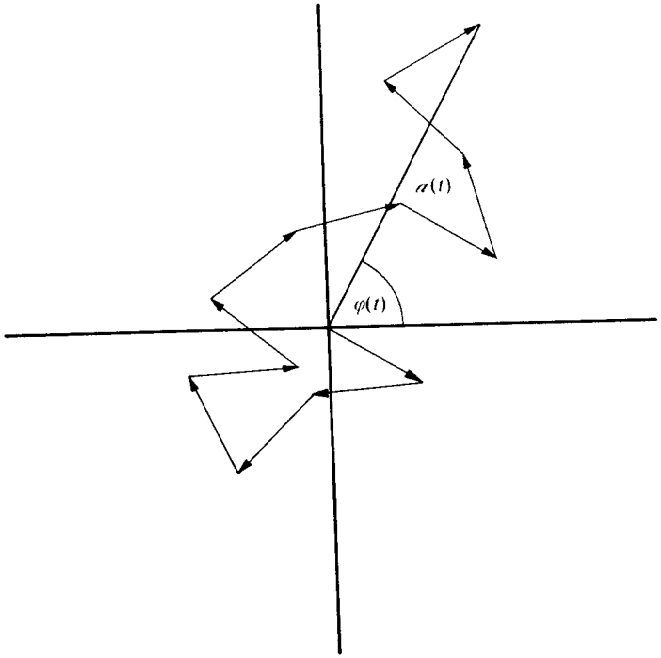

FIG. 3.3. Argand diagram to show the amplitude $a(t)$ and phase $\varphi(t)$ of the resultant vector formed by a large number of unit vectors, each of which has a randomly chosen phase angle.

frequency ω_0 given in eqn (1.65). It is therefore appropriate for comparison with experiment to average the theoretical results over a cycle of oscillation of the carrier wave. The real electric field from eqn (3.14) has a zero cycle-average. According to eqn (1.89), the cycle average of the beam intensity in free space is

$$\bar{I}(t) = \tfrac{1}{2}\epsilon_0 c|E(t)|^2 = \tfrac{1}{2}\epsilon_0 c E_0^2 a(t)^2. \tag{3.15}$$

The intensity $\bar{I}(t)$ still contains the time dependence resulting from the random amplitude modulation $a(t)$.

Figs. 3.4 and 3.5 illustrate the types of fluctuation that occur in the beam intensity and phase. The figures have been constructed by a computer simulation of a collision-broadened light source in which the summation of phase factors in eqn (3.14) is carried out explicitly for a large number of atoms ν. The phase variation for each atom has the form shown in Fig. 3.2 with free-flight times distributed in accordance with the probability law of eqn (2.131). The horizontal time-scales for both $\bar{I}(t)$ and $\varphi(t)$ in Figs. 3.4 and 3.5 are determined solely by the magnitude of the mean time τ_0 of free flight indicated

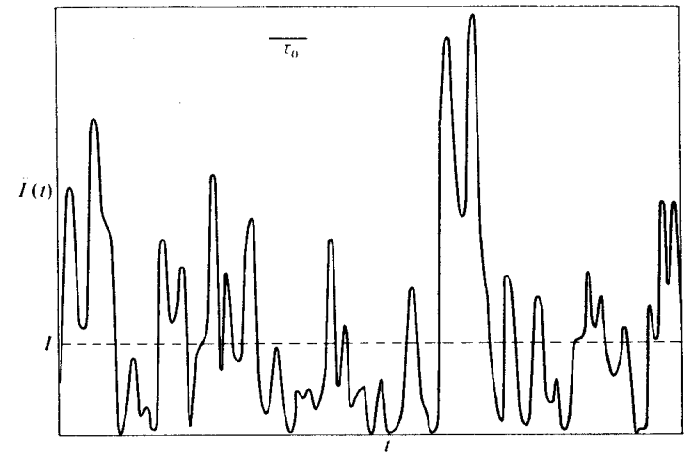

FIG. 3.4. Time dependence of the cycle-averaged intensity for a chaotic light beam, obtained from a computer simulation. The mean time τ_0 between collisions has the magnitude indicated. The dashed line shows the mean value of the intensity averaged over a time long compared to τ_0. (Computation carried out by Mrs S. Sussmann.)

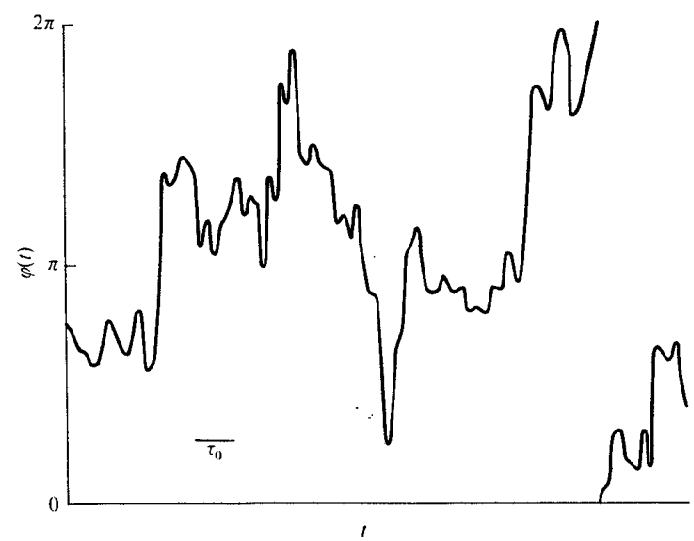

FIG. 3.5. Time dependence of the phase of the wave emitted by a collision-broadened source. The graph is a result of the same computation that produced Fig. 3.4.

on the graphs. It is seen that substantial changes in intensity and phase can occur over a time span τ_0, but that these quantities are reasonably constant over time intervals $\Delta t \ll \tau_0$.

The inclusion of radiative and Doppler broadening would modify the details of the above discussion but the fluctuations in intensity and phase remain similar to those illustrated in Figs. 3.4 and 3.5. For any combination of line-broadening mechanisms there exists some characteristic time, analogous to τ_0 in the collision-broadening case, which determines the time-scale of the random fluctuations. This characteristic time is called, in general, the *coherence time* τ_c of the light beam. Its magnitude is of the order of the inverse of the frequency spread of the beam. The relevance of τ_c to the usual definition of coherence is discussed later in the chapter.

In all the theory that follows, attention is restricted to light beams whose frequency spreads are small compared with the mean frequency, that is, where $\omega_0\tau_c$ is very much larger than unity. It is seen from Fig. 1.6 that the light generated by thermal excitation of a cavity (the black-body radiation) has a frequency spread nearly equal to the mean frequency and does not fall into this category.

The path length

$$\lambda_c = c\tau_c \tag{3.16}$$

associated with the coherence time is known as the *coherence length*. The graph of the cycle-averaged intensity as a function of time at a fixed point in the beam given in Fig. 3.4 could equally well be regarded as a graph of the intensity as a function of the distance z along the beam at a fixed instant of time. The horizontal axis would be relabelled z and the mean time τ_0 would be relabelled λ_c. At a given instant of time, the cycle-averaged intensity changes only slightly over distances that are small compared to λ_c, but large changes occur over distances that are comparable to or larger than λ_c. The temporal and spatial aspects of the beam fluctuations are related by the simple scaling factor c. The coherence length for the beams considered is always much larger than the wavelength of the light.

3.3. First-order coherence and frequency spectrum

The model of a collision-broadened light source described above can be used to calculate the first-order electric-field correlation function of the light, its degree of first-order coherence, and its frequency spectrum.

Consider first the correlation function of the fields at different times, defined by the time average in eqn (3.4). It is clear from the discussion of Figs. 3.4 and 3.5 that the electric field $E(t)$ changes little over periods much smaller than the coherence time, but that large changes occur over periods much longer than

the coherence time. The fields at times separated by such long periods are essentially uncorrelated. The time average in eqn (3.4) depends only on the characteristics of the light and is independent of the sampling time T if the latter extends over many coherence times. In addition, it is assumed that the theory refers to an experiment that is capable of resolving the fluctuation properties; the detector resolving time must therefore be much smaller than τ_c, and its dimension parallel to the beam must be much smaller than λ_c.

These are the conditions for use of the ergodic theorem to evaluate the correlation function (3.4). The angle brackets are thus interpreted as a statistical average, and the required function is

$$\begin{aligned}\langle E^*(t)E(t+\tau)\rangle &= E_0^2 \exp(-\mathrm{i}\omega_0\tau)\langle\{\exp(-\mathrm{i}\phi_1(t))+\ldots+\exp(-\mathrm{i}\phi_\nu(t))\}\\ &\quad\times\{\exp(\mathrm{i}\phi_1(t+\tau))+\ldots+\exp(\mathrm{i}\phi_\nu(t+\tau))\}\rangle,\end{aligned} \tag{3.17}$$

where eqn (3.14) has been used. In multiplying out the large brackets, the phase angles of the wave trains from different atoms have different random values and the cross-terms give a zero average contribution. The remaining terms give

$$\begin{aligned}\langle E^*(t)E(t+\tau)\rangle &= E_0^2 \exp(-\mathrm{i}\omega_0\tau)\sum_{i=1}^{\nu}\langle\exp[\mathrm{i}(\phi_i(t+\tau)-\phi_i(t))]\rangle\\ &= \nu\langle E_i^*(t)E_i(t+\tau)\rangle\end{aligned} \tag{3.18}$$

since all the radiating atoms are equivalent.

The correlation function for the beam as a whole is thus determined by the single-atom contributions. Now the phase angle of each wave train jumps to a random value after its atom suffers a collision, subsequently producing a zero average contribution. Thus the single-atom correlation function in eqn (3.18) is proportional to the probability that the atom has a period of free flight longer than τ, and with use of the probability distribution (2.131) we can put

$$\begin{aligned}\langle E_i^*(t)E_i(t+\tau)\rangle &= E_0^2 \exp(-\mathrm{i}\omega_0\tau)\langle\exp[\mathrm{i}(\phi_i(t+\tau)-\phi_i(t))]\rangle\\ &= E_0^2 \exp(-\mathrm{i}\omega_0\tau)\int_\tau^\infty p(\tau)\,\mathrm{d}\tau\\ &= E_0^2 \exp\{-\mathrm{i}\omega_0\tau-(\tau/\tau_0)\}.\end{aligned} \tag{3.19}$$

The correlation function (3.18) thus becomes

$$\langle E^*(t)E(t+\tau)\rangle = \nu E_0^2 \exp\{-\mathrm{i}\omega_0\tau-(\tau/\tau_0)\} \tag{3.20}$$

and the normalized correlation or degree of first-order coherence (3.8) is

$$g^{(1)}(\tau) = \exp\{-\mathrm{i}\omega_0\tau-(\tau/\tau_0)\}. \tag{3.21}$$

The spectrum of the collision-broadened light is obtained by integration of the degree of first-order coherence as in eqn (3.11) to give

$$F(\omega) = \frac{1/\pi\tau_0}{(\omega_0-\omega)^2+(1/\tau_0)^2}. \tag{3.22}$$

This is a normalized Lorentzian lineshape similar to eqn (2.112). The linewidth $2/\tau_0$ agrees with that in eqn (2.140) when radiative broadening is ignored if

$$\gamma_{\text{coll}} = 1/\tau_0, \tag{3.23}$$

as assumed without proof in eqn (2.133). The degree of first-order coherence can thus be written

$$g^{(1)}(\tau) = \exp(-i\omega_0\tau-\gamma_{\text{coll}}\tau). \tag{3.24}$$

The degree of first-order coherence and the spectrum in the presence of both collision and radiative broadening can be calculated by a generalization of the model of the light source[1]. It is found that the results are much the same as above except that γ_{coll} must be augmented by addition of the radiative damping parameter γ to form the total damping γ' defined in eqn (2.135). Thus the correlation function and degree of first-order coherence are generalized to

$$\langle E^*(t)E(t+\tau)\rangle = \nu E_0^2 \exp(-i\omega_0\tau-\gamma'\tau) \tag{3.25}$$

and

$$g^{(1)}(\tau) = \exp(-i\omega_0\tau-\gamma'\tau). \tag{3.26}$$

The spectrum is a Lorentzian with width (2.140), and the coherence time is

$$\tau_c = 1/\gamma'. \tag{3.27}$$

The effect of Doppler broadening on the coherence is considered in §3.5.

We note that the correlations in any kind of chaotic light must vanish for times τ much longer than τ_c, and since

$$\langle E(t)\rangle = 0, \tag{3.28}$$

it follows that the degree of first-order coherence must have a limiting value

$$g^{(1)}(\tau) \to 0 \qquad \text{for} \qquad \tau \gg \tau_c. \tag{3.29}$$

Apart from its usefulness in deriving the frequency spectrum of the light, the degree of first-order coherence plays a more direct role in determining the results of interference experiments. It is convenient to illustrate the role by consideration of a specific experiment.

3.4. Young's interference fringes

Young's fringes provide a simple example of an interference experiment, and their treatment illustrates some general principles that are common to the

whole class of experiments. The experiment is here analysed in some detail to determine the conditions under which the field fluctuations, resulting from the chaotic nature of the light source, affect the visibility of the interference fringes. Fig. 3.6 shows a simplified version of Young's experiment. Chaotic light from a point source is rendered parallel by a lens and then falls on a screen that contains two slits, or pinholes as we shall assume for simplicity. Interference fringes are sought on a second screen placed to the right of the first screen. The model experiment ignores complications arising from the finite source diameter and consequent lack of perfect parallelism in the beam that illuminates the first screen. It is essential to take such effects into account in a rigorous treatment of the experiment but they are omitted here in order that attention can be focused on the effects of the random field fluctuations alone.

Let $E(\mathbf{r}t)$ be the total electric field of the radiation at the position $\mathbf{r}$ on the observation screen at time t. The field is a linear superposition of the electric fields at the two pinholes (positions $\mathbf{r}_1$ and $\mathbf{r}_2$) at earlier times t_1 and t_2 determined by the velocity of light c. Thus formally,

$$E(\mathbf{r}t) = u_1E(\mathbf{r}_1t_1)+u_2E(\mathbf{r}_2t_2), \tag{3.30}$$

where

$$t_1 = t-(s_1/c), \qquad t_2 = t-(s_2/c), \tag{3.31}$$

and the coefficients u_1, u_2 are inversely proportional to s_1, s_2, respectively, the distances defined in Fig. 3.6. The coefficients u_1 and u_2 depend on the geometry of the experiment, for example on the pinhole sizes, but their exact form is not important for the present calculation; they are purely imaginary, since the secondary waves radiated by the pinholes are $\pi/2$ out of phase with the primary light beam[2]. Diffraction effects at the individual pinholes are ignored.

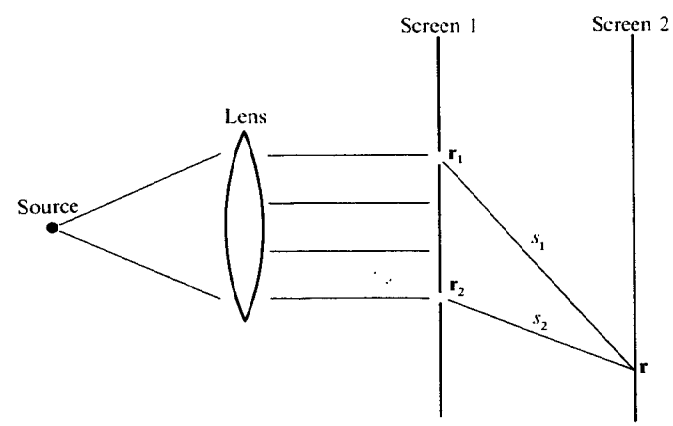

FIG. 3.6. Arrangement of components for an idealized Young's interference experiment.

The intensity of the light at position **r**, averaged over a cycle of oscillation, is

$$\begin{aligned}\bar{I}(\mathbf{r}t) &= \tfrac{1}{2}\epsilon_0 c|E(\mathbf{r}t)|^2 \\ &= \tfrac{1}{2}\epsilon_0 c\{|u_1|^2|E(\mathbf{r}_1t_1)|^2+|u_2|^2|E(\mathbf{r}_2t_2)|^2 \\ &\quad +2u_1^*u_2\,\mathrm{Re}(E^*(\mathbf{r}_1t_1)E(\mathbf{r}_2t_2))\},\end{aligned} \tag{3.32}$$

where the pure imaginary form of u_1 and u_2 has been used. The intensity $\bar{I}(\mathbf{r}t)$ is similar to that defined in eqn (3.15).

The fringes in Young's interference experiment are normally recorded by photographic plates or are observed with the naked eye. In either case, the recording time is long compared to τ_c, the coherence time of the chaotic light. To compare theory with experiment it is necessary to average $\bar{I}(\mathbf{r}t)$ over a period long compared with τ_c. This average of $\bar{I}(\mathbf{r}t)$ is denoted $\bar{I}(\mathbf{r})$, and the averaged form of eqn (3.32) is then

$$\begin{aligned}\bar{I}(\mathbf{r}) &= \langle\bar{I}(\mathbf{r}t)\rangle \\ &= \tfrac{1}{2}\epsilon_0 c\{|u_1|^2\langle|E(\mathbf{r}_1t_1)|^2\rangle+|u_2|^2\langle|E(\mathbf{r}_2t_2)|^2\rangle \\ &\quad +2u_1^*u_2\,\mathrm{Re}\langle E^*(\mathbf{r}_1t_1)E(\mathbf{r}_2t_2)\rangle\}.\end{aligned} \tag{3.33}$$

It is seen that the intensity on the second screen consists of three contributions. The first two terms represent the intensities caused by each of the pinholes in the absence of the other. These two terms do not give rise to any interference effects. The fringes arise from the term that involves the correlation function for the fields at the two pinholes.

The correlation function is a slight generalization of that defined in eqn (3.4) to take account of the different spatial positions of the two fields. The formal definition is

$$\langle E^*(\mathbf{r}_1t_1)E(\mathbf{r}_2t_2)\rangle = \frac{1}{T}\int_T E^*(\mathbf{r}_1t_1)E(\mathbf{r}_2t_1+t_{21})\,\mathrm{d}t_1, \tag{3.34}$$

where

$$t_{21} = t_2-t_1. \tag{3.35}$$

The required correlation function is in fact less general than this because the light beam that strikes the first screen in Young's experiment is assumed to be parallel and to have plane wave-fronts.

Let the direction of propagation of the beam be taken as the z-axis. The electric field of the light can be represented as in eqn (3.14) except that the position dependence must now be included. The light beam with its fluctuations travels along the z-axis at velocity c, and the position-dependent field is accordingly

$$E(zt) = E\left(t-\frac{z}{c}\right), \tag{3.36}$$

where the field on the right is the same as in eqn (3.14). The calculation of the correlation function now proceeds as in eqns (3.17)–(3.20) and the result is essentially the same as before except that now

$$\tau = t_2-\frac{z_2}{c}-t_1+\frac{z_1}{c}. \tag{3.37}$$

With this definition, the generalization of eqn (3.25) is

$$\langle E^*(z_1t_1)E(z_2t_2)\rangle = vE_0^2\exp(-\mathrm{i}\omega_0\tau-\gamma'\tau). \tag{3.38}$$

The fringe intensity in Young's experiment is determined by substitution of eqn (3.38) into eqn (3.33). The two pinholes have the same z coordinate, and the intensity reduces to

$$\bar{I}(\mathbf{r}) = \tfrac{1}{2}\epsilon_0 cE_0^2v\{|u_1|^2+|u_2|^2+2u_1^*u_2\exp(-\gamma'|\tau|)\cos\omega_0\tau\}, \tag{3.39}$$

where τ, determined from eqns (3.31) and (3.37), is

$$\tau = (s_1-s_2)/c. \tag{3.40}$$

This quantity can be either positive or negative and the use of $|\tau|$ in the exponential in eqn (3.39) accords with the symmetry property of eqn (3.10). The fringe visibility at position **r** on the second screen is conventionally defined to be

$$\frac{\bar{I}(\mathbf{r})_{\max}-\bar{I}(\mathbf{r})_{\min}}{\bar{I}(\mathbf{r})_{\max}+\bar{I}(\mathbf{r})_{\min}} = \frac{2u_1^*u_2\exp(-\gamma'|s_1-s_2|/c)}{|u_1|^2+|u_2|^2}. \tag{3.41}$$

The fringe visibility is unity at the centre of the second screen in Fig. 3.6, where $u_1 = u_2$ and $s_1 = s_2$, but is less than unity off the axis, where $u_1 \neq u_2$ and $s_1 \neq s_2$.

The chaotic nature of the light source influences the fringe visibility via the exponential term in eqn (3.41) which, in principle, causes the fringes to disappear altogether for s_1 sufficiently different from s_2. However, it is seen from eqn (3.39) that for a narrow emission line, where $\omega_0 \gg \gamma'$, very many fringes are generated by the cosine term before τ becomes sufficiently large for the exponential term to blur the fringes. For the coherence time and frequency assumed in eqns (2.141) and (1.65), there are about 10^4 sharp fringes on the second screen centred about the axis of the experiment. In a practical Young's interference experiment the chaotic nature of the light is not usually the most important cause of fringe blurring. The finite extent of the source perpendicular to the axis, neglected in the above treatment, is often the most important limiting factor, and there are, in fact, techniques for determining the angular diameters of distant light sources, for example stars, by observation of fringe blurring[3]. Source-size effects belong to the theory of spatial coherence considered briefly in §3.9.

The chaotic properties of the light source assumed in the interference fringe calculation thus have very little effect on the results of experiments that use suitably narrow emission lines. The exponential factors in eqns (3.39) and (3.41) would however be of great importance in attempts to observe fringes with light from a broad-band source, for example a thermal cavity where the frequency spread of the light is comparable to its mean frequency. At the opposite extreme, the above treatment of interference is inappropriate for an emission line so narrow that the time-dependent intensity fluctuations are observed directly. However, the longest coherence time ordinarily available for a chaotic source is of order 10^{-9} s, and the experimental resolving time in interference experiments is usually much longer than τ_c.

The important feature of the above treatment is the way in which the formation of fringes is governed by the first-order electric-field correlation function. The correlation function plays a similar role in other classical interference experiments, for example the Michelson interferometer.

3.5. Degree of first-order coherence

The properties of a light beam that are relevant to an interference experiment can be conveniently expressed in terms of the concept of optical coherence. Light at two points in space or time that is capable, in principle, of being superimposed to produce interference effects is said to be coherent. An example is the light at the two pinholes in Young's interference experiment. The potential magnitude of the interference effects in most of the classical interference experiments is governed by the first-order coherence of the light beam employed.

The degree of first-order temporal coherence is defined as the normalized electric-field correlation function, similar to eqn (3.8). However, we now generalize the previous definition to include the spatial dependence of the electric fields. The degree of first-order temporal coherence between the light fields at the space–time points $(\mathbf{r}_1, t_1)$ and $(\mathbf{r}_2, t_2)$ is defined to be

$$g^{(1)}(\mathbf{r}_1 t_1, \mathbf{r}_2 t_2) = \frac{\langle E^*(\mathbf{r}_1 t_1) E(\mathbf{r}_2 t_2)\rangle}{[\langle |E(\mathbf{r}_1 t_1)|^2\rangle \langle |E(\mathbf{r}_2 t_2)|^2\rangle]^{\frac{1}{2}}} \tag{3.42}$$

where the angle brackets again denote statistical averages. The light at the two points has the following designations that depend upon the value of the degree of first-order coherence.

$$\text{For} \quad |g^{(1)}(\mathbf{r}_1 t_1, \mathbf{r}_2 t_2)| \begin{cases} = 1 \\ = 0 \\ \neq 0 \text{ or } 1 \end{cases} \quad \text{the light is} \begin{cases} \text{first-order coherent} \\ \text{incoherent} \\ \text{partially coherent.} \end{cases} \tag{3.43}$$

The examples to be treated here all involve plane parallel light beams where only a single spatial coordinate, taken as the z-axis, is needed. Consider first the chaotic light source of Lorentzian frequency distribution assumed above for the theory of Young's experiment. The required correlation function given by eqn (3.38) contains the positions and times only in the combination τ defined in eqn (3.37). It is therefore convenient to introduce a shorthand for the degree of coherence, writing

$$g^{(1)}(z_1 t_1, z_2 t_2) \equiv g^{(1)}(\tau) = \exp(-\mathrm{i}\omega_0 \tau - \gamma' |\tau|). \tag{3.44}$$

The result is formally identical to eqn (3.26) except that the symmetry (3.10) is used to include both positive and negative τ. The dependence of $|g^{(1)}(\tau)|$ on τ is shown in Fig. 3.7. The light at the two points is first-order coherent if

$$|t_2 - t_1 - (z_2 - z_1)/c| \ll \tau_c, \tag{3.45}$$

where eqn (3.27) has been used. In Young's experiment, where $z_1 = z_2$, sharp fringes occur provided that the two sets of wavelets, which impinge at a point on the second screen, left the pinholes at times separated by an amount small compared to the coherence time, where τ_c is typically of order 3×10^{-11} s according to eqn (2.141). The corresponding coherence length is about 10^{-2} m. It is possible to form interference fringes in general from a parallel beam of light only by superposition of light from two points whose distances along the beam differ by less than the coherence length, and which leaves the two points at times that differ by less than the coherence time.

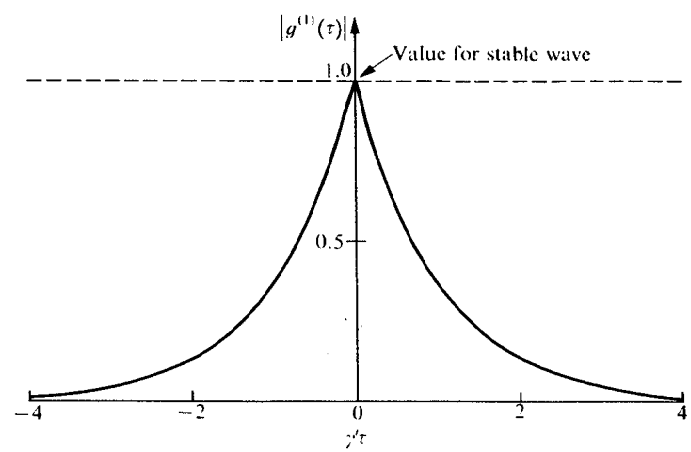

FIG. 3.7. The modulus of the degree of first-order coherence for chaotic light of linewidth parameter γ'. The constant unit value for a classical stable wave is indicated by the dashed line.

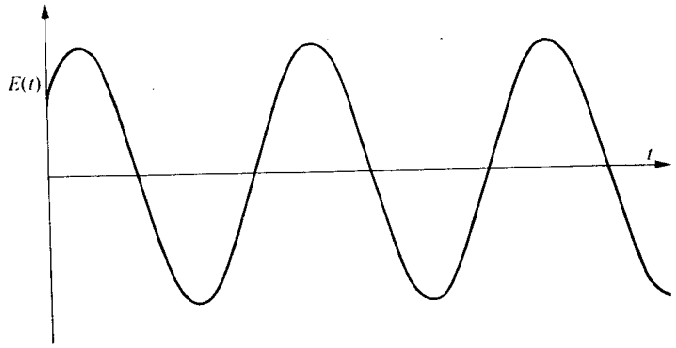

FIG. 3.8. Variation of electric field with time at a fixed observation point for a classical stable wave.

All of the above analysis is based on the assumption of a collision-broadened light source. It is not difficult to evaluate the degree of first-order coherence for other kinds of light. The simplest example of all is provided by the classical wave of stable amplitude and phase that is often assumed in the theoretical treatment of optical experiments. For such a wave, assumed to be propagated in the z-direction, the electric field can be written

$$E(zt) = E_0 \exp(ikz - i\omega_0 t + i\phi), \tag{3.46}$$

where the amplitude and phase are fixed quantities, in contrast to the chaotic field of eqn (3.14), and the wavevector is $k = \omega_0/c$. Fig. 3.8 shows the variation of electric field with time at a fixed observation point. The first-order correlation function is determined without any ensemble averaging in this case, since the field has no statistical uncertainty, and

$$\langle E^*(z_1 t_1) E(z_2 t_2)\rangle = E_0^2 \exp(-i\omega_0 \tau), \tag{3.47}$$

with τ given by eqn (3.37). Thus, from eqn (3.42), the first-order coherence is

$$g^{(1)}(\tau) = \exp(-i\omega_0 \tau). \tag{3.48}$$

The beam is first-order coherent at all space–time points and it can be said to have perfect first-order coherence. The result (3.48) is the same as obtained by letting the linewidth parameter γ' tend to zero in the chaotic beam result (3.44) (or equivalently $\tau_c \to \infty$). The stable-wave result is also shown in Fig. 3.7. As is discussed in Chapter 7, the beam from a single-mode laser source can approximate a noiseless classical stable wave of the kind shown in Fig. 3.8.

Between the two extremes of the chaotic beam and the classical stable wave, there are other examples of light beam whose first-order coherence can be

easily evaluated. These examples give insight into the conditions required to obtain coherent light.

Problem 3.1. Consider a one-dimensional cavity that contains a chaotic light beam, and suppose that all the cavity-mode contributions to the field except one are removed by means of a filter. The mode that remains has a large number of contributions similar to the stable wave of Fig. 3.8, all with the same frequency and wavevector but with a random distribution of phase angles. Prove that the beam is first-order coherent at any pair of space–time points in the cavity.

Problem 3.2. Consider the beam of light produced by excitation of two stable waves where the electric field is

$$E(zt) = E_1 \exp(ik_1 z - i\omega_1 t) + E_2 \exp(ik_2 z - i\omega_2 t). \tag{3.49}$$

Prove that the beam of light is first-order coherent at all pairs of points.

These are examples of some general conditions under which light can have perfect first-order coherence. The conditions are satisfied if either (1) only a single cavity mode is excited, or (2) the field can be specified precisely, with no statistical features. If the beam involves excitation of more than one mode *and* exhibits statistical fluctuations, it is not possible for the light to be first-order coherent at all pairs of space–time points.

Problem 3.3. Consider a beam of light produced by excitation of two modes as in eqn (3.49), but where both modes exhibit random phase and amplitude fluctuations. If the average intensity is equally divided between the modes, prove that

$$|g^{(1)}(\tau)| = \cos\{\tfrac{1}{2}(\omega_1 - \omega_2)\tau\}. \tag{3.50}$$

As a final topic in first-order coherence theory, we return to the case of a chaotic light source but now consider the degree of coherence that results when Doppler broadening is the main cause of the spread in emission frequencies. The emission lineshape is the same as that in absorption, given by eqn (2.153). If all other sources of line-broadening are ignored, the total electric field of the radiated light beam at a fixed observation point can be written

$$E(t) = E_0 \sum_{i=1}^{\nu} \exp(-i\omega_i t + i\phi_i), \tag{3.51}$$

where E_0 and ϕ_i are the fixed amplitude and phase of the wave train radiated by the ith atom. Different atoms have different frequencies ω_i of radiation that are Doppler-shifted from ω_0 by an amount depending on the atomic velocity.

The first-order electric-field correlation function is written with the help of eqns (3.36) and (3.51) as

$$\langle E^*(z_1t_1)E(z_2t_2)\rangle = E_0^2 \sum_{i,j=1}^{\nu} \left\langle \exp\left\{ i\omega_i\left(t_1-\frac{z_1}{c}\right)+i\phi_i - i\omega_j\left(t_2-\frac{z_2}{c}\right)-i\phi_j\right\}\right\rangle. \tag{3.52}$$

The phase angles have fixed values but are randomly distributed, and the contributions for $i \neq j$ average to zero, leaving

$$\langle E^*(z_1t_1)E(z_2t_2)\rangle = E_0^2 \sum_{i=1}^{\nu} \exp(-i\omega_i\tau), \tag{3.53}$$

where τ is defined in eqn (3.37). The sum that remains is converted to an integration over the Gaussian distribution of Doppler-shifted frequencies given in eqn (2.153),

$$\langle E^*(z_1t_1)E(z_2t_2)\rangle = \nu E_0^2(2\pi\delta^2)^{-\frac{1}{2}}\int_0^\infty \exp(-i\omega_i\tau)\exp\{-(\omega_i-\omega_0)^2/2\delta^2\}\,d\omega_i$$
$$= \nu E_0^2 \exp(-i\omega_0\tau-\tfrac{1}{2}\delta^2\tau^2). \tag{3.54}$$

This result is the analogue for Doppler-broadened light of the correlation function (3.38) for collision- and radiatively-broadened light.

The corresponding degree of first-order coherence is

$$g^{(1)}(\tau) = \exp(-i\omega_0\tau-\tfrac{1}{2}\delta^2\tau^2). \tag{3.55}$$

The coherence time in this case is

$$\tau_c \approx 1/\delta \tag{3.56}$$

and it has the same qualitative significance as the coherence time for light of Lorentzian frequency distribution. The modulus of the degree of first-order coherence (3.55) is illustrated in Fig. 3.9.

Problem 3.4. Consider light from a source that simultaneously has some Lorentzian broadening with parameter γ' and some Gaussian broadening with parameter δ. Prove that the degree of first-order coherence is

$$g^{(1)}(\tau) = \exp(-i\omega_0\tau-\gamma'|\tau|-\tfrac{1}{2}\delta^2\tau^2). \tag{3.57}$$

In the treatment of simultaneous collision and Doppler broadening it is assumed here, as in §2.13, that the two mechanisms are independent.

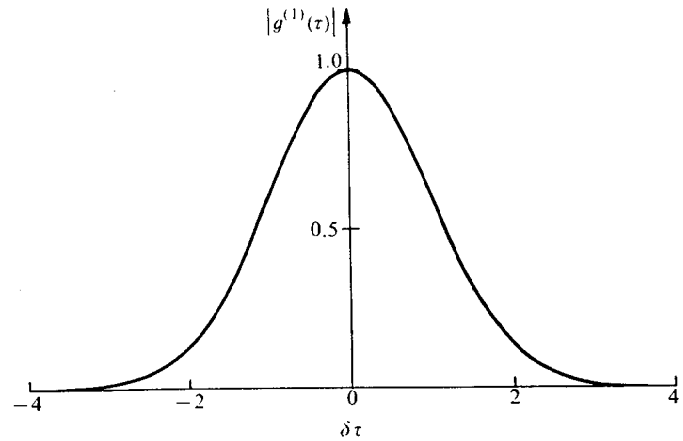

FIG. 3.9. The modulus of the degree of first-order coherence for chaotic light of Gaussian frequency distribution with root-mean-square width δ. Compare with Fig. 3.7 for the Lorentzian frequency distribution.

3.6. Intensity fluctuations of chaotic light

The present chapter has so far been concerned almost exclusively with the fluctuations in the electric field of a chaotic light beam. The main outcome of the theory is the first-order electric-field correlation function and its normalized version, the degree of first-order temporal coherence. We have seen how these functions determine the formation of fringes in the classical interference experiments.

The second main topic of the chapter concerns the direct measurement of intensity fluctuations of the kind shown in Fig. 3.4. We describe the measurement of higher-order interference effects that depend upon the correlations of two *intensities* at different times rather than the correlations of two *fields*. The results of such measurements are governed by the degree of second-order temporal coherence of the light.

As a preliminary to the discussion of intensity interference experiments, the present section considers the statistical properties of the intensity fluctuations in chaotic light. In many cases the fluctuations in the cycle-averaged intensity are too rapid for direct observation, and what is measured is some average of the fluctuations over the detector response time. We suppose initially however that there is available an ideal detector, with response time much shorter than the coherence time τ_c, that can take effectively instantaneous measurements of the intensity.

The average value of a large number of measurements of the cycle-averaged intensity $\bar{I}(t)$ taken over a period of time very much longer than τ_c is easy to

calculate. With the long observation period and the assumption of instantaneous intensity measurements, the conditions for application of the ergodic theorem are satisfied, and its validity is assumed throughout the present section. The time average can thus be replaced by a statistical average over the distribution of phase angles, denoted by angle brackets. From eqns (3.14) and (3.15) the long-time average intensity is

$$\begin{aligned}\bar{I} \equiv \langle \bar{I}(t)\rangle &= \tfrac{1}{2}\epsilon_0 c E_0^2 \langle |\exp(\mathrm{i}\phi_1(t)) + \exp(\mathrm{i}\phi_2(t)) + \ldots + \exp(\mathrm{i}\phi_\nu(t))|^2\rangle \\ &= \tfrac{1}{2}\epsilon_0 c E_0^2 \nu, \end{aligned} \tag{3.58}$$

since the cross-terms between the phase factors for different radiating atoms give zero average contributions. The value of $\bar{I}$ for the fluctuating intensity illustrated in Fig. 3.4 is indicated by the dashed horizontal line. This average intensity is the quantity that is ordinarily used in theories of light transmission through absorbing media, as in Chapter 1.

The average values of higher powers of the cycle-averaged intensity can be calculated in a similar fashion. Thus the mean square intensity is

$$\langle \bar{I}(t)^2\rangle = \tfrac{1}{4}\epsilon_0^2 c^2 E_0^4 \langle |\exp(\mathrm{i}\phi_1(t)) + \exp(\mathrm{i}\phi_2(t)) + \ldots + \exp(\mathrm{i}\phi_\nu(t))|^4\rangle. \tag{3.59}$$

In taking the average of the fourth power of the sum of phase factors, the only non-zero terms are those in which each factor is multiplied by its complex conjugate. These terms give

$$\begin{aligned}\langle \bar{I}(t)^2\rangle &= \tfrac{1}{4}\epsilon_0^2 c^2 E_0^4 \Big\{ \sum_i \langle |\exp(\mathrm{i}\phi_i(t))|^4\rangle \\ &\qquad + \sum_{i\neq j} \langle |2\exp[\mathrm{i}(\phi_i(t)+\phi_j(t))]|^2\rangle \Big\} \\ &= \tfrac{1}{4}\epsilon_0^2 c^2 E_0^4 \{\nu + 2\nu(\nu-1)\}. \end{aligned} \tag{3.60}$$

Thus in terms of the average intensity given by eqn (3.58), the mean-square intensity is

$$\langle \bar{I}(t)^2\rangle = \left(2 - \frac{1}{\nu}\right)\bar{I}^2. \tag{3.61}$$

The number ν of radiating atoms is normally very large and eqn (3.61) can then be written

$$\langle \bar{I}(t)^2\rangle = 2\bar{I}^2 \qquad (\nu \gg 1) \tag{3.62}$$

to a very good approximation.

The root-mean-square deviation of the cycle-averaged intensity is

$$(\langle \bar{I}(t)^2\rangle - \langle \bar{I}(t)\rangle^2)^{\frac{1}{2}} = \bar{I}. \tag{3.63}$$

The size of fluctuation is thus equal to the average intensity, as is qualitatively evident in Fig. 3.4. A similar result was found in eqns (1.41) or (1.42) for the

fluctuations in number of the thermally excited photons in a single cavity mode.

The averages of higher powers of $\bar{I}(t)$ than the second are quite complicated in general, but relatively simple results are obtained if the number of radiating atoms is assumed to be very large. Then as in the second moment calculation in eqn (3.60) the dominant contribution comes from terms that involve the square modulus of products of the phase factors of distinct atoms. The approximate average of the rth power of the intensity is

$$\begin{aligned}\langle \bar{I}(t)^r\rangle &= (\tfrac{1}{2}\epsilon_0 c E_0^2)^r \sum_{\substack{i,j,k,\ldots \\ (r\text{ different atoms})}}{}' \langle |r!\exp[\mathrm{i}(\phi_i(t)+\phi_j(t)+\phi_k(t)+\ldots)]|^2\rangle \\ &= (\tfrac{1}{2}\epsilon_0 c E_0^2)^r\, {}^\nu C_r (r!)^2. \end{aligned} \tag{3.64}$$

Thus with ν assumed very much larger than r and the average intensity taken from eqn (3.58),

$$\langle \bar{I}(t)^r\rangle = r!\bar{I}^r \qquad (\nu \gg r). \tag{3.65}$$

This result for the rth moment of the intensity fluctuation distribution, although derived here for the collision-broadened source, is in fact valid for any kind of chaotic light. The occurrence of the $r!$ factor in eqn (3.65) is a distinctive feature of chaotic light. The similarity to the rth factorial moment (1.38) for the thermal photon distribution should be noted.

Provided that the number of radiating atoms is very large, it is possible to calculate not only the moments derived above but also the explicit form of the probability distribution for the cycle-averaged intensity. The first step is the determination of the statistical distribution of the values of $a(t)$.

It is seen from eqn (3.14) and Fig. 3.3 that at any instant of time t, $a(t)$ is the distance from the origin in an Argand diagram arrived at by taking ν steps of unit length and in random directions specified by the angles $\phi_1(t), \phi_2(t), \ldots, \phi_\nu(t)$. The calculation is an example of the 'random walk' problem, well known in the theory of stochastic processes[4]. Let $p[a(t)]$ be the probability that the end-point of a random walk of ν steps lies in unit area around the point specified by coordinates $a(t)$, $\varphi(t)$ in Fig. 3.3. The result given by random-walk theory for the present problem is[5]

$$p[a(t)] = (1/\pi\nu)\exp(-a(t)^2/\nu), \tag{3.66}$$

being independent of $\varphi(t)$ as expected from the physical nature of the problem. The probability is normalized,

$$\int_0^\infty \mathrm{d}a(t) \int_0^{2\pi} a(t)p[a(t)]\,\mathrm{d}\varphi(t) = 1. \tag{3.67}$$

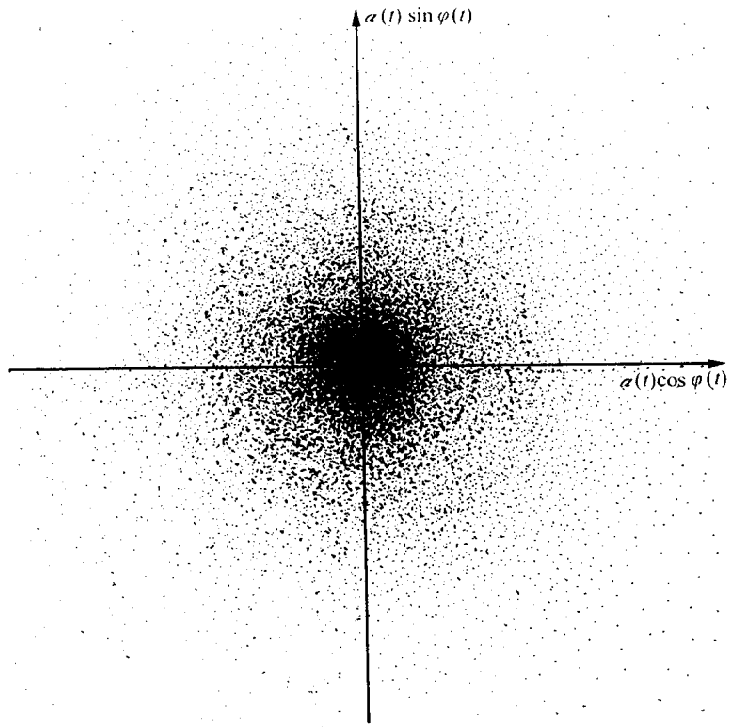

FIG. 3.10. Probability distribution for the amplitude and phase of the electric field of a chaotic light beam. The density of shading is proportional to the probability at the point in the plane corresponding to polar coordinates $\alpha(t)$ and $\varphi(t)$. Note that the probability is greatest at the origin and is independent of $\varphi(t)$.

The probability distribution (eqn (3.66)) is a Gaussian function, whose form is shown in Fig. 3.10. A similar distribution arises for any chaotic light beam, and because of this the light from a chaotic source is sometimes called Gaussian light. It is important not to confuse the Gaussian distribution of $|E(t)|$ with the distribution of frequencies in the beam, which can be Lorentzian, Gaussian, or an intermediate function, and is indeed Lorentzian for the collision-broadening mechanism assumed here.

The probability distribution for $\alpha(t)$ can be converted to a probability distribution for $\bar{I}(t)$ with the help of eqn (3.15).

Problem 3.5. Prove that the probability for an instantaneous measurement of the cycle-averaged intensity to yield a value between $\bar{I}(t)$ and $\bar{I}(t)+\mathrm{d}\bar{I}(t)$ is $p[\bar{I}(t)]\,\mathrm{d}\bar{I}(t)$, where

$$p[\bar{I}(t)] = (1/\bar{I})\exp(-\bar{I}(t)/\bar{I}), \tag{3.68}$$

and $\bar{I}$ is given by eqn (3.58). Note that the most probable value of $\bar{I}(t)$ is always zero.

The random-walk probability distribution strictly refers to the results of a large number of walks that all begin at the origin. For the problem in hand, the end-point of each walk defines an amplitude α and a phase φ for a light beam. Random-walk theory assigns a certain probability to every possible α and φ. The collection of light beams with all possible amplitudes and phases forms a statistical ensemble of the type mentioned in §1.4. Each light beam in the ensemble has fixed α and φ, and the intensity distribution shown in eqn (3.68) is rigorously valid for such an ensemble of fixed-amplitude and fixed-phase beams. Its application to determine time averages of a long series of instantaneous intensity measurements on a single beam of chaotic light relies once more on the ergodic theorem. The moments of the distribution (3.68), given by

$$\langle \bar{I}(t)^r \rangle = (1/\bar{I})\int_0^\infty \bar{I}(t)^r \exp(-\bar{I}(t)/\bar{I})\,\mathrm{d}\bar{I}(t) = r!\,\bar{I}^r, \tag{3.69}$$

agree with the result (3.65) obtained previously.

All of the above results refer to idealized experiments that measure the instantaneous intensity. The effects of a finite detector response time, particularly on the second moment of the intensity fluctuations, are discussed in §3.9. At the extreme limit of a very long coherence time, it is possible by somewhat artificial means to construct a light beam in which the intensity fluctuations are easily visible. Such a beam can be generated[6] by the scattering of laser light from small polystyrene balls suspended in water. Small Doppler shifts of the scattered frequency result from the Brownian motion of the balls. The suspension is a slowed-down analogue of a radiating gas, with the sharp laser frequency replacing the atomic transition frequency. The coherence time τ_c is of order 10^{-1} s, and the intensity fluctuations are apparent to the naked eye.

A contrast to the above results for chaotic light is provided by the classical stable wave of Fig. 3.8. There is no need to employ statistics in this case; the cycle-averaged intensity is constant and there are no intensity fluctuations. The result analogous to eqn (3.65) is

$$\langle \bar{I}(t)^r \rangle = \bar{I}^r, \tag{3.70}$$

and the root-mean-square deviation is zero.

3.7. Degree of second-order coherence

The intensity-fluctuation properties of chaotic light described in the previous section refer to averages of intensity readings taken at single instants of

time. We now consider two-time measurements in which a series of pairs of intensity readings are taken with a fixed time-delay τ. The average of the product of each pair of intensity readings is the intensity correlation function of the light, analogous to the electric-field correlation function defined in eqn (3.4). The measurement of intensity correlations is described in §3.9; we here consider the theory of the correlation function.

It is convenient to work with a normalized form of the correlation function called the *degree of second-order temporal coherence*,

$$g^{(2)}(\tau) = \frac{\langle \bar{I}(t)\bar{I}(t+\tau)\rangle}{\bar{I}^2} = \frac{\langle E^*(t)E^*(t+\tau)E(t+\tau)E(t)\rangle}{\langle E^*(t)E(t)\rangle^2}, \tag{3.71}$$

where $\bar{I}$ is the average intensity defined as in eqn (3.58), and the order of electric-field factors in the second-order electric-field correlation function follows a convention. It is clear from the symmetry of the definition that the property analogous to eqn (3.10) is

$$g^{(2)}(-\tau) = g^{(2)}(\tau), \tag{3.72}$$

and calculations need only be made for positive τ. It is assumed that the measurements are made at a fixed point in space and satisfy the conditions for equivalence of statistical and time averages as before.

We have seen that the degree of first-order coherence takes values in the range 0 to 1, and it might be expected at first sight that the degree of second-order coherence would have a similar range. This is not however correct. The allowed range of values of the degree of second-order coherence is controlled by two inequalities; both are based on Cauchy's inequality[7], according to which two measurements of the intensity at times t_1 and t_2 must satisfy

$$2\bar{I}(t_1)\bar{I}(t_2) \leqslant \bar{I}(t_1)^2 + \bar{I}(t_2)^2. \tag{3.73}$$

By applying this inequality to the cross-terms, it is easy to show that

$$\left\{\frac{\bar{I}(t_1)+\bar{I}(t_2)+\ldots+\bar{I}(t_N)}{N}\right\}^2 \leqslant \frac{\bar{I}(t_1)^2+\bar{I}(t_2)^2+\ldots+\bar{I}(t_N)^2}{N} \tag{3.74}$$

for the results of N measurements of the intensity. Thus in the correlation function notation,

$$\bar{I}^2 \equiv \langle \bar{I}(t)\rangle^2 \leqslant \langle \bar{I}(t)^2\rangle, \tag{3.75}$$

and the zero time-delay degree of second-order coherence from eqn (3.71) satisfies

$$g^{(2)}(0) \geqslant 1. \tag{3.76}$$

It is not possible to establish any upper limit, and the complete range is given by

$$\infty \geqslant g^{(2)}(0) \geqslant 1. \tag{3.77}$$

The above proof cannot be extended to finite time delays, and the only restriction then results from the essentially positive nature of the intensity, which gives

$$\infty \geqslant g^{(2)}(\tau) \geqslant 0 \qquad \tau \neq 0. \tag{3.78}$$

There is however another important property that follows from the inequality

$$[\bar{I}(t_1)\bar{I}(t_1+\tau)+\ldots+\bar{I}(t_N)\bar{I}(t_N+\tau)]^2 \leqslant [\bar{I}(t_1)^2+\ldots+\bar{I}(t_N)^2][\bar{I}(t_1+\tau)^2+\ldots+\bar{I}(t_N+\tau)^2], \tag{3.79}$$

which is also readily established with the help of eqn (3.73). The two summations on the right of eqn (3.79) are equal for a sufficiently long and numerous series of measurements, and the square root then produces the result

$$\langle \bar{I}(t)\bar{I}(t+\tau)\rangle \leqslant \langle \bar{I}(t)^2\rangle, \tag{3.80}$$

or

$$g^{(2)}(\tau) \leqslant g^{(2)}(0). \tag{3.81}$$

These general properties of the degree of second-order coherence are illustrated by the example shown in Fig. 3.11. Part (a) of the figure shows a train of rectangular classical pulses of duration τ_0. Suppose that the intensity I_0 within each pulse is constant and that the duration and separation of the pulses give a mean intensity that can be written

$$\bar{I} = fI_0 \qquad 0 < f \leqslant 1. \tag{3.82}$$

Here f is the number of pulses per unit time multiplied by τ_0. It is a trivial exercise to show from eqn (3.71) that

$$g^{(2)}(0) = 1/f, \tag{3.83}$$

and only a brief calculation is needed to verify the time dependence of the degree of second-order coherence shown in part (b) of Fig. 3.11. The degree of coherence correctly satisfies the inequalities (3.77) and (3.81), and indeed the zero time-delay value (3.83) covers the whole range allowed by eqn (3.77) for the different choices of f.

The special case of a beam of constant intensity I_0 is obtained for $f = 1$, when it is easily shown that

$$g^{(2)}(\tau) = 1, \tag{3.84}$$

independent of the time delay τ. This is the case of a classical stable wave, and for $\tau = 0$ eqn (3.84) agrees with the result obtained from eqn (3.70).

3.8. Second-order coherence of chaotic light

The statistical properties of chaotic light produce beam intensities that are uncorrelated after time separations long compared to the coherence time τ_c.

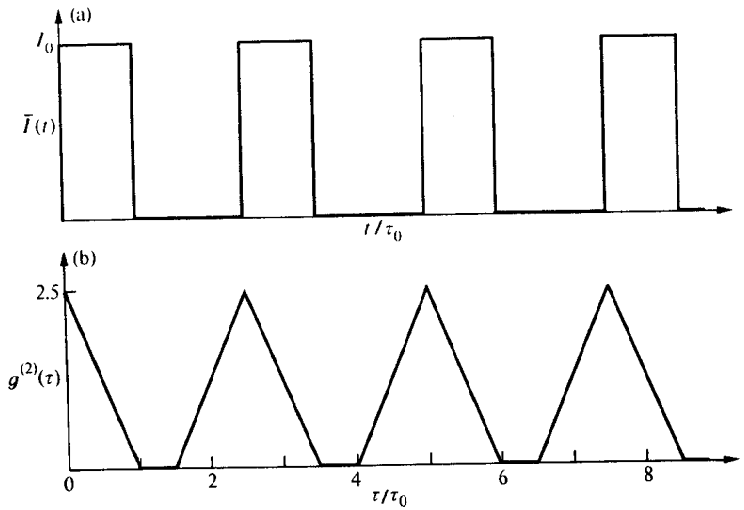

FIG. 3.11. (a) Intensity variation for a train of rectangular pulses of duration τ_0 and separation $1{\cdot}5\tau_0$, giving $f = 0{\cdot}4$. (b) The corresponding degree of second-order coherence.

The degree of second-order coherence (3.71) thus has a limiting value

$$g^{(2)}(\tau) \to 1 \qquad \text{for} \qquad \tau \gg \tau_c, \tag{3.85}$$

in contrast to the zero limiting value of the degree of first-order coherence given in eqn (3.29). The regular wave train of Fig. 3.11 has an infinitely long coherence time and the limit does not apply in this case.

In order to determine the degree of second-order coherence of chaotic light we suppose, as in the models used earlier in the present chapter for both collision and Doppler-broadened light, that the electric field of the light beam is made up of independent contributions from the different radiating atoms i,

$$E(t) = \sum_i E_i(t). \tag{3.86}$$

The second-order electric-field correlation function that appears in eqn (3.71) is thus

$$\begin{aligned}\langle E^*(t)E^*(t+\tau)E(t+\tau)E(t)\rangle &= \sum_{i=1}^{v} \langle E_i^*(t)E_i^*(t+\tau)E_i(t+\tau)E_i(t)\rangle \\ &\quad + \sum_{i\neq j}\{\langle E_i^*(t)E_j^*(t+\tau)E_j(t+\tau)E_i(t)\rangle \\ &\quad + \langle E_i^*(t)E_j^*(t+\tau)E_i(t+\tau)E_j(t)\rangle\},\end{aligned} \tag{3.87}$$

where only those terms are retained in which the field of each atom is multiplied by its complex conjugate. All other terms vanish because of the random relative phases of the waves from different atoms. Thus taking account of the equivalence of the contribution from each atom

$$\begin{aligned}\langle E^*(t)E^*(t+\tau)E(t+\tau)E(t)\rangle &= v\langle E_i^*(t)E_i^*(t+\tau)E_i(t+\tau)E_i(t)\rangle \\ &\quad + v(v-1)\{\langle E_i^*(t)E_i(t)\rangle^2 + |\langle E_i^*(t)E_i(t+\tau)\rangle|^2\}.\end{aligned} \tag{3.88}$$

If the number v of radiating atoms is now assumed to be very large, the contributions that involve pairs of atoms greatly exceed the single-atom contributions, and to a good approximation

$$\langle E^*(t)E^*(t+\tau)E(t+\tau)E(t)\rangle = v^2\{\langle E_i^*(t)E_i(t)\rangle^2 + |\langle E_i^*(t)E_i(t+\tau)\rangle|^2\}. \tag{3.89}$$

The corresponding result for the first-order electric-field correlation function is given in eqn (3.18). Thus with the definitions (3.8) and (3.71) of the degrees of first- and second-order coherence, eqns (3.18) and (3.89) give

$$g^{(2)}(\tau) = 1 + |g^{(1)}(\tau)|^2 \qquad (v \gg 1). \tag{3.90}$$

This important relation holds for all varieties of chaotic light.

The second-order electric-field correlation function in eqn (3.88) can be explicitly evaluated for the model of a collision-broadened light-source used to evaluate the first-order correlation function (3.25). The only additional result needed is

$$\langle E_i^*(t)E_i^*(t+\tau)E_i(t+\tau)E_i(t)\rangle = E_0^4, \tag{3.91}$$

and eqn (3.88) then gives

$$\langle E^*(t)E^*(t+\tau)E(t+\tau)E(t)\rangle = vE_0^4 + v(v-1)E_0^4\{1+\exp(-2\gamma'\tau)\}. \tag{3.92}$$

Thus with the help of eqn (3.25), the degree of second-order coherence (3.71) is

$$g^{(2)}(\tau) = \frac{1}{v} + \left(1 - \frac{1}{v}\right)\{1+\exp(-2\gamma'\tau)\}, \tag{3.93}$$

in agreement at $\tau = 0$ with the zero time-delay degree of second-order coherence obtained from eqn (3.61). The degree of coherence at negative τ is obtained from the symmetry property (3.72), and in the limit of a large number of radiating atoms, eqn (3.93) gives

$$g^{(2)}(\tau) = 1 + \exp(-2\gamma'|\tau|) \qquad (v \gg 1), \tag{3.94}$$

in agreement with the general result (3.90).

Fig. 3.12 shows the form of the degree of second-order coherence for the chaotic light of Lorentzian frequency distribution assumed in the derivation of

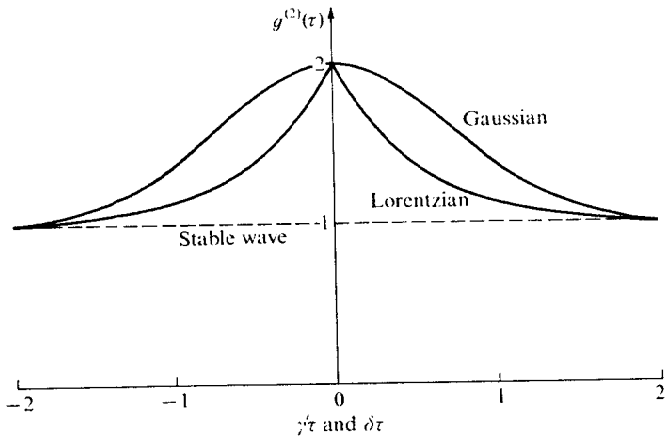

FIG. 3.12. The degrees of second-order coherence of chaotic light having Gaussian and Lorentzian frequency distributions with linewidth parameters δ and γ' respectively. The dashed line shows the constant unit second-order coherence of a classical stable wave.

eqn (3.94). The corresponding result for chaotic light of Gaussian frequency distribution,

$$g^{(2)}(\tau) = 1+\exp(-\delta^2\tau^2), \tag{3.95}$$

obtained from eqns (3.55) and (3.90) is also illustrated. The stable-wave result (3.84) is indicated by the horizontal dashed line. All three examples in the figure satisfy the general inequalities (3.77) and (3.81), and both kinds of chaotic light have the limiting value (3.85). It is evident from eqn (3.90) that

$$g^{(2)}(0) = 2 \tag{3.96}$$

for any kind of chaotic light since $g^{(1)}(0) = 1$ from its definition (3.8). This result is also evident from eqn (3.69).

The peak in the degree of second-order coherence of chaotic light for $\tau < \tau_c$ is a manifestation of the kind of intensity fluctuations shown in Fig. 3.4. For such small delay times, the two intensity measurements to be correlated in the degree of second-order coherence can fall within the same fluctuation peak to give an enhanced contribution. For longer delay-times, $\tau > \tau_c$, the two intensities tend to be uncorrelated and the degree of second-order coherence is close to unity.

The degrees of second-order coherence calculated above assume a polarized beam of light and a fixed observation point. The definition (3.71) can be generalized, analogous to eqn (3.42), to include the spatial dependence of the optical fields. The degree of second-order temporal coherence between the

light at space-time points $(\mathbf{r}_1, t_1)$ and $(\mathbf{r}_2, t_2)$ is defined to be

$$g^{(2)}(\mathbf{r}_1t_1,\mathbf{r}_2t_2;\mathbf{r}_2t_2,\mathbf{r}_1t_1) = \frac{\langle E^*(\mathbf{r}_1t_1)E^*(\mathbf{r}_2t_2)E(\mathbf{r}_2t_2)E(\mathbf{r}_1t_1)\rangle}{\langle|E(\mathbf{r}_1t_1)|^2\rangle\langle|E(\mathbf{r}_2t_2)|^2\rangle}, \tag{3.97}$$

where the angle brackets again denote ensemble averages. Note that this function is a special case of a more general second-order coherence in which the four fields in the correlation function are evaluated at four different space–time points, but we do not consider this further generalization. The light at points $(\mathbf{r}_1, t_1)$ and $(\mathbf{r}_2, t_2)$ is said to be second-order coherent if simultaneously

$$\left.\begin{aligned} |g^{(1)}(\mathbf{r}_1t_1,\mathbf{r}_2t_2)| &= 1 \\ g^{(2)}(\mathbf{r}_1t_1,\mathbf{r}_2t_2;\,\mathbf{r}_2t_2,\mathbf{r}_1t_1) &= 1. \end{aligned}\right\} \tag{3.98}$$

The inclusion of spatial dependence in the degree of second-order coherence is here restricted to plane-polarized parallel beams of light where only the single z-coordinate is needed. Then, as in the discussion of first-order coherence, the spatial dependence of the field is incorporated via eqn (3.36) and it is not difficult to verify that, analogous to eqn (3.44),

$$g^{(2)}(z_1t_1,z_2t_2;\,z_2t_2,z_1t_1) = g^{(2)}(\tau), \tag{3.99}$$

where τ is defined in eqn (3.37). With this interpretation of τ, the expressions already derived for the degree of second-order coherence apply to spatially separated points in the parallel beam.

As discussed in connection with eqn (3.44), chaotic light is always first-order coherent for space–time points sufficiently close together. This is illustrated by the approach of the first-order coherence of the chaotic light in Figs. 3.7 and 3.9 towards unity for small $\gamma'\tau$ or $\delta\tau$. However, the small τ limit produces a second-order coherence of 2 according to eqn (3.96), as illustrated in Fig. 3.12. It is not possible for chaotic light to be second-order coherent in accordance with the definition (3.98) for any choice of space–time points. By contrast, eqns (3.48) and (3.84) show that the classical stable wave is second-order coherent at all space–time points.

Problem 3.6. Consider the single-mode chaotic light beam, defined in problem 3.1 as a randomly-phased superposition of stable waves. Prove from first principles that

$$g^{(2)}(\tau) = 2. \tag{3.100}$$

The coherence time is infinite in this case and eqn (3.85) does not apply.

3.9. Experiment of Hanbury Brown and Twiss

The results of all the classical interference experiments, typified by Young's slits, are controlled by the correlation of two electric-field amplitudes,

conveniently expressed in terms of the degree of first-order coherence of the light. The correlation of two optical intensities, conveniently expressed in terms of the degree of second-order coherence, was first measured by Hanbury Brown and Twiss[8,9], Their experiment typifies all subsequent measurements of degrees of second-order coherence. Such measurements have a particular significance in terms of the correspondence between the classical and quantum theories of light. We here consider the classical theory of the experiment, reserving the quantum discussion for Chapter 6, where the theory of optical coherence is reconsidered in terms of the quantized radiation field.

The experimental apparatus is shown schematically in Fig. 3.13. Light from a mercury arc is filtered to eliminate all but the 435·8-nm emission line of the mercury spectrum. The beam is split into two equal portions by a half-silvered mirror. The intensity of each portion is measured by a photomultiplier detector, the principles of which are outlined in §5.6, and the fluctuations in the outputs of the two detectors are multiplied together in the correlator. The integrated value of this product over a long period of observation provides a measurement of the magnitude of the intensity fluctuations.

One of the detectors is mounted on a slide so that its position can be varied laterally relative to the fixed detector. This enables the detector apertures as viewed from the pinhole to be superimposed or completely separated and provides a verification of the reality of the observed fluctuations, which must vanish for sufficient detector separation. Let us ignore this feature of the experiment and treat an idealized arrangement in which the two detectors are symmetrically placed with respect to the mirror. They then measure the intensities in the beams at equal linear distances z from the light source.

According to the classical theory, the half-silvered mirror divides the incident cycle-averaged intensity $\bar{I}(zt)$ into two identical beams in arms 1 and 2

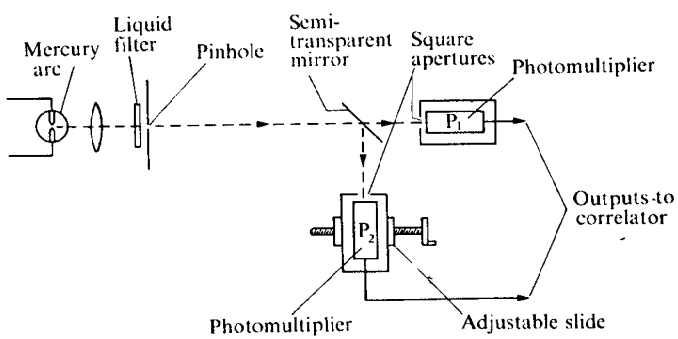

FIG. 3.13. Arrangement of the main components in an intensity interference experiment. (After R. Hanbury Brown and R. Q. Twiss, ref. 8.)

of the experiment. In an obvious notation we can write

$$\bar{I}_1(zt) = \bar{I}_2(zt) = \tfrac{1}{2}\bar{I}(zt), \tag{3.101}$$

and the long-time average intensities in the two arms are

$$\bar{I}_1 = \bar{I}_2 = \tfrac{1}{2}\bar{I}. \tag{3.102}$$

We ignore until later the complications introduced by the finite response times of the detectors, and assume that the experiment is capable of correlating the intensities at the two detectors measured instantaneously at different times t_1 and t_2. The correlator was designed to produce the average

$$\langle[\bar{I}_1(zt_1)-\bar{I}_1][\bar{I}_2(zt_2)-\bar{I}_2]\rangle = \tfrac{1}{4}\{\langle\bar{I}(zt_1)\bar{I}(zt_2)\rangle-\bar{I}^2\}. \tag{3.103}$$

The normalized version of the Hanbury Brown and Twiss correlation is readily expressed in terms of the degree of second-order coherence,

$$\frac{\langle[\bar{I}_1(zt_1)-\bar{I}_1][\bar{I}_2(zt_2)-\bar{I}_2]\rangle}{\bar{I}_1\bar{I}_2} = g^{(2)}(\tau)-1, \tag{3.104}$$

where in this case $\tau = t_2-t_1$.

It is seen therefore that apart from a normalization factor the experiment of Hanbury Brown and Twiss measures the deviation from unity of the degree of second-order coherence. The results of the experiment can be envisaged in terms of the examples shown in Fig. 3.12. Only chaotic light was available at the time of the original experiments; in this case the correlation (3.104) is unity for $\tau \ll \tau_c$ but falls to zero for $\tau \gg \tau_c$. Similar experiments have since been made on light that closely corresponds to the classical stable wave; in this case the Hanbury Brown and Twiss correlation is zero for all values of τ.

For chaotic light of Lorentzian frequency distribution, the correlation given by (3.94) and (3.104) is

$$g^{(2)}(\tau)-1 = \exp(-2\gamma'|t_2-t_1|). \tag{3.105}$$

This is however not a realistic prediction for the correlation expected in a practical experiment, where it is never possible to make instantaneous measurements of the beam intensity. There is always some minimum response time τ_r of the detection system such that the recorded intensity is a mean over the period τ_r. Consider a Hanbury Brown and Twiss experiment where the 'instantaneous' intensities are measured simultaneously by two detectors of equal response time τ_r. If the additional average over the detector response time is indicated by further angle brackets, the predicted result is

$$\begin{aligned}\langle g^{(2)}(\tau)\rangle_r-1 &= \frac{1}{\tau_r^2}\int_0^{\tau_r}\mathrm{d}t_1\int_0^{\tau_r}\exp(-2\gamma'|t_2-t_1|)\,\mathrm{d}t_2\\ &= (1/2\gamma'^2\tau_r^2)\{\exp(-2\gamma'\tau_r)-1+2\gamma'\tau_r\}.\end{aligned} \tag{3.106}$$

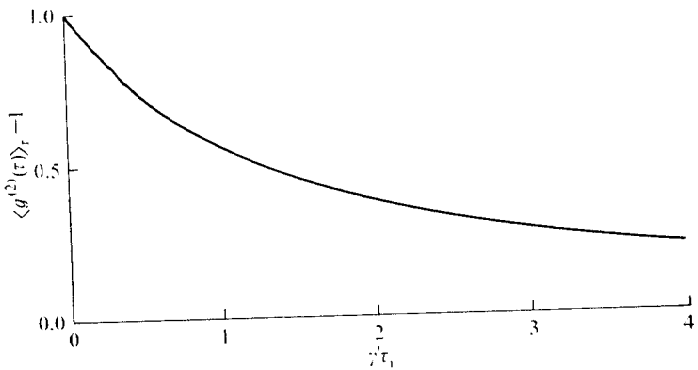

FIG. 3.14. Magnitude of the correlated intensity fluctuations of chaotic light having a Lorentzian frequency distribution with linewidth parameter γ'. Both detectors have response time τ_r.

This result is illustrated in Fig. 3.14.

For a very short detector response time where

$$\gamma'\tau_r \ll 1 \quad \text{or} \quad \tau_r \ll \tau_c, \tag{3.107}$$

the right-hand side of eqn (3.106) reduces to unity, in agreement with the result (3.105) in the case of simultaneous measurement of the instantaneous intensities. In the opposite limit of a long response time, where

$$\gamma'\tau_r \gg 1 \quad \text{or} \quad \tau_r \gg \tau_c, \tag{3.108}$$

eqn (3.106) gives

$$\langle g^{(2)}(\tau)\rangle_r - 1 = 1/\gamma'\tau_r = \tau_c/\tau_r; \tag{3.109}$$

the magnitude of the observed intensity fluctuations, inversely proportional to the response time, is seriously reduced in this case. Note that the final form of the reduction factor in eqn (3.109) applies whether or not the chaotic light has a Lorentzian frequency distribution. The original measurements[8] were carried out with a light source and detection equipment for which the reduction factor was as high as 10^5, and the success of the experiment depended upon the processing of the measured intensities to obtain the correlated intensity fluctuations (3.104) directly.

The intensity interference effects described above depend on the second-order *temporal coherence* of the light. However the practical observation of the intensity correlations is also affected by the *spatial coherence* of the light, associated with the finite dimensions of the source and the detectors. The corresponding effects of spatial coherence in first-order interference experiments have been mentioned in the discussion of Young's slits. The spatial coherence is not of great interest here since it is not so intrinsic a property of

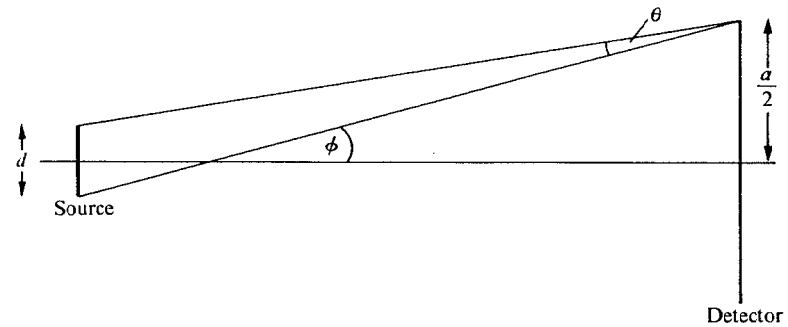

FIG. 3.15. Arrangement of source and detector for the consideration of spatial coherence.

the light as the temporal coherence. However, it is of course of great importance in the design of interference experiments and we briefly consider it.

Fig. 3.15 shows a light source of finite dimension d perpendicular to the axis of an optical experiment, in which the light is collected by a detector that also has finite dimensions perpendicular to the axis. The linear dimensions of source and detector are assumed to be very small compared to their separation. The phases of the light from different parts of the source have a varying relation across the detector. There is a 180° phase difference between light from the two ends of the source at a point in the detector distance $a/2$ off the axis if

$$\phi d = \tfrac{1}{2}\lambda, \tag{3.110}$$

where ϕ is the angle defined in Fig. 3.15 and λ is the wavelength of the light. Thus

$$a = 2\phi d/\theta = \lambda/\theta, \tag{3.111}$$

where θ is the angular diameter of the source viewed from the detector.

The dimension a gives a rough measure of the size of detector for which the desired field or intensity correlations begin to suffer diminutions as a result of cancellations between the contributions of different parts of the detector. The experiments of Hanbury Brown and Twiss used light with a wavelength of about 4×10^{-7} m and their light source had an angular diameter of about 8×10^{-5} rad viewed from the detectors. Their detector dimension of 5 mm thus satisfied the condition (3.111), and the spatial coherence effects caused only a modest reduction in the size of the observed intensity fluctuations. It is seen that the spatial coherence controls the phase variation of the light in a direction perpendicular to the beam and is determined by the closeness of the light beam to the ideal of plane parallelism. The temporal coherence controls the fluctuation and correlation properties of the fields and intensities of the light in a direction parallel to the beam, and is determined by the properties of the light-emitting atoms in the source[10].

Although the temporal coherence properties of light are of most interest for the present account, it must be emphasized that the main interest of Hanbury Brown and Twiss was in spatial coherence effects. Thus the purpose of the adjustable slide shown in Fig. 3.13 was to allow the spatial separation of the two detectors as viewed from the source by distances exceeding the spatial coherence length (3.111). The observed fall-off in the correlation between the intensities recorded in the two detectors allows an experimental determination of the angular diameter θ of the source. The laboratory experiment illustrated in Fig. 3.13 was a prototype for a large-scale optical intensity-interferometer that has been most successfully used in measuring the angular diameters of stars[9].

Returning now to the discussion of temporal coherence, it is clear from expressions given earlier in the present section that intensity-interference experiments can be used to determine the coherence time and hence the linewidth parameter of the light source. Because of the inverse relation between these quantities, a narrow emission line corresponds to a relatively long time scale for the intensity fluctuations. Thus determinations of linewidths by study of intensity fluctuations tend to be feasible for just those sources whose frequency spreads are so narrow that conventional frequency-domain spectroscopy is incapable of resolving them. Time-domain spectroscopy is considered further in Chapter 6, where the effects of quantization of the radiation field are also included.

3.10. Higher-order coherence and polarization effects

The degrees of first-and second-order coherence defined by eqns (3.42) and (3.97) are just the first two members of a hierarchy of coherence functions. It is possible to envisage a general interference experiment in which the measured result depends on the correlations of electric fields at an arbitrary number of space–time points. The result of any such measurement depends upon the hierarchy of coherence functions in some way. The degree of rth-order coherence can be defined as[11]

$$g^{(r)}(\mathbf{r}_1t_1,\ldots,\mathbf{r}_rt_r;\,\mathbf{r}_{r+1}t_{r+1},\ldots,\mathbf{r}_{2r}t_{2r}) = \frac{\langle E^*(\mathbf{r}_1t_1)\ldots E^*(\mathbf{r}_rt_r)E(\mathbf{r}_{r+1}t_{r+1})\ldots E(\mathbf{r}_{2r}t_{2r})\rangle}{(\langle|E(\mathbf{r}_1t_1)|^2\rangle\ldots\langle|E(\mathbf{r}_rt_r)|^2\rangle\langle|E(\mathbf{r}_{r+1}t_{r+1})|^2\rangle\ldots\langle|E(\mathbf{r}_{2r}t_{2r})|^2\rangle)^{\frac{1}{2}}}. \tag{3.112}$$

Clearly, eqns (3.42) and (3.97) are special cases of this general definition.

It is not intended to pursue the general rth-order coherence properties of light in any detail, since the first- and second-order coherence are usually of greatest experimental importance. However, it is worth noting two simple

results. When the points $(\mathbf{r}_{r+1}t_{r+1}),\ldots,(\mathbf{r}_{2r}t_{2r})$ are the same as the points $(\mathbf{r}_rt_r),\ldots,(\mathbf{r}_1t_1)$, the correlation function in eqn (3.112) effectively contains the intensities at r different points. For the classical stable wave, the same arguments as are used for obtaining $g^{(2)}$ show that

$$g^{(r)}(\mathbf{r}_1t_1,\ldots,\mathbf{r}_rt_r;\,\mathbf{r}_rt_r,\ldots,\mathbf{r}_1t_1) = 1 \text{ for all } r. \tag{3.113}$$

By an obvious extension of the definition of second-order coherence in eqn (3.98), the classical stable wave can be said to be coherent in all orders.

There is no similarly simple result for a chaotic light beam, but the very special case where *all* the points in eqn (3.112) are the same space–time point $(\mathbf{r}_1t_1)$ can be quoted, since the correlation function is then the same as that evaluated in eqn (3.65), and

$$g^{(r)}(\mathbf{r}_1t_1,\ldots,\mathbf{r}_1t_1;\,\mathbf{r}_1t_1,\ldots,\mathbf{r}_1t_1) = r!. \tag{3.114}$$

Problem 3.7. Consider the rectangular pulse beam shown in Fig. 3.11. Prove that the rth-order coherence at a single space–time point $(\mathbf{r}_1t_1)$ is

$$g^{(r)}(\mathbf{r}_1t_1,\ldots,\mathbf{r}_1t_1;\,\mathbf{r}_1t_1,\ldots,\mathbf{r}_1t_1) = f^{-r+1}. \tag{3.115}$$

The result shows that $g^{(r)}$ can take any arbitrarily large value by choosing f sufficiently small, except for $r = 1$ where the degree of first-order coherence is unity, independent of f.

The entire chapter has been concerned with a beam of polarized light and the electric fields have been treated as scalar quantities. We conclude the discussion of intensity fluctuations of chaotic light with a brief consideration of the changes in some of the simpler results that occur when the beam is not plane polarized.[12]

Consider a beam of light propagated parallel to the z-axis that is made up of two independent beams, one of mean intensity $\bar{I}_x$ polarized parallel to the x-axis and one of mean intensity $\bar{I}_y$ polarized parallel to the y-axis. The total mean intensity is

$$\bar{I} = \bar{I}_x + \bar{I}_y \tag{3.116}$$

and the degree of polarization is defined to be

$$P = \frac{\bar{I}_x - \bar{I}_y}{\bar{I}_x + \bar{I}_y} \qquad (\bar{I}_x \geqslant \bar{I}_y), \tag{3.117}$$

where the x-axis is chosen to be that with the larger mean intensity. Thus $P = 1$ corresponds to polarized light and $P = 0$ to unpolarized light, with intermediate values of P corresponding to partially polarized light.

For chaotic light, the two independent beams have cycle-averaged fluctuating intensities $\bar{I}_x(t)$ and $\bar{I}_y(t)$ that both obey the exponential probability distribution (3.68). The total intensity $\bar{I}(t)$, obtained by adding the two

contributions, thus follows the probability distribution

$$p[\bar{I}(t)] = \int_0^{\bar{I}(t)} p_x[\bar{I}_x(t)]\, p_y[\bar{I}(t)-\bar{I}_x(t)]\, \mathrm{d}\bar{I}_x(t), \tag{3.118}$$

where

$$p_{x,y}[\bar{I}_{x,y}(t)] = (1/\bar{I}_{x,y})\exp(-\bar{I}_{x,y}(t)/\bar{I}_{x,y}). \tag{3.119}$$

The integration is readily carried out to give

$$p[\bar{I}(t)] = (1/P\bar{I})\{\exp[-2\bar{I}(t)/(1+P)\bar{I}] - \exp[-2\bar{I}(t)/(1-P)\bar{I}]\}. \tag{3.120}$$

Fig. 3.16 shows the form of the probability distribution for several degrees of polarization. The general expression (3.120) reduces to eqn (3.68) in the limit $P = 1$ of plane polarization. However, the probability is zero at $\bar{I}(t) = 0$ for all other degrees of polarization. The distributions corresponding to several values of P have been measured and the experimental results agree with the theoretical expressions.[13–15]

Problem 3.8. Derive the average value of the rth power of the cycle-averaged intensity for partially polarized chaotic light and show that it has the limiting values

$$\begin{aligned} \langle \bar{I}(t)^r \rangle &= r!\,\bar{I}^r && \text{for} \quad P = 1 \\ &= (r+1)!\,\bar{I}^r/2^r && \text{for} \quad P = 0. \end{aligned} \tag{3.121}$$

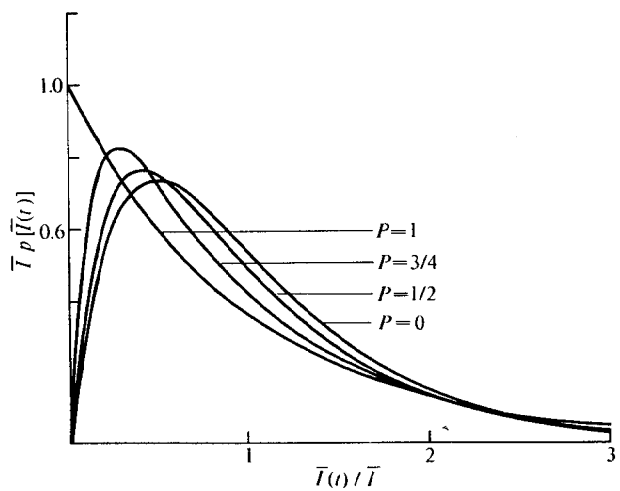

FIG. 3.16. Probability distributions for the cycle-averaged intensities of chaotic light with various degrees of polarization P. (After L. Mandel, ref. 12.)

Show that the zero time-delay degree of second-order coherence of the light is

$$g^{(2)}(0) = \tfrac{1}{2}(3+P^2). \tag{3.122}$$

This last result reduces to eqn (3.96) for polarized light but otherwise has a smaller value. Its form can be understood if it is rewritten as

$$g^{(2)}(0) = 1+\tfrac{1}{2}(1+P^2) = 1+(\bar{I}_x/\bar{I})^2+(\bar{I}_y/\bar{I})^2, \tag{3.123}$$

where eqns (3.116) and (3.117) have been used. Then with reference to Fig. 3.12, the unit term is the background contribution that occurs even in the absence of any fluctuations. The fluctuations cause the remaining terms, whose contribution is generally smaller than unity because there are no cross-correlations between the x- and y- polarized beams. With unpolarized light the fluctuation contribution to $g^{(2)}(0)$ is $\frac{1}{2}$; the theory of the Hanbury Brown and Twiss experiment given above remains valid if $\frac{1}{2}$ factors are substituted in appropriate places.

References

1. Simultaneous radiative and collision broadening is briefly considered by PARK, D. (1971). *Am. J. Phys.* **39,** 682.
2. See, for example, BORN, M. and WOLF, E. (1970). *Principles of optics*, p. 374. Pergamon, Oxford.
3. See p. 271 of ref. 2.
4. WAX, N. (Ed.) (1954). *Selected papers on noise and stochastic processes* Dover, New York.
5. CHANDRASEKHAR, S. (1943). *Rev. Mod. Phys.* **15,** 1. Reprinted in ref. 4.
6. PIKE, E. R. (1970). In *Quantum optics* (eds. S. M. Kay and A. Maitland), p. 127. Academic Press, New York.
7. HARDY, G. H., LITTLEWOOD, J. E., and PÓLYA, G. (1951). *Inequalities*. Cambridge University Press.
8. HANBURY BROWN, R. and TWISS, R. Q. (1956). *Nature* **177,** 27; (1957). *Proc. R. Soc.* **A242,** 300; (1958) *ibid.* **A243,** 291.
9. An interesting account of the original experiments and of their development for measurements of stellar diameters is given by HANBURY BROWN, R. (1974). *The intensity interferometer*. Taylor and Francis, London.
10. A most useful collection of original papers on all aspects of coherence theory is MANDEL, L. and WOLF, E. (Eds.) (1970). *Selected papers on coherence and fluctuations of light*, Vols. 1 and 2. Dover, New York.
11. GLAUBER, R. J. (1965). *Quantum optics and electronics* (eds. C. DeWitt, A. Blandin, and C. Cohen-Tannoudji), p. 63. Gordon and Breach, New York. (1970). *Quantum optics* (eds. S. M. Kay and A. Maitland), p. 53. Academic Press, New York.
12. MANDEL, L. (1963). *Proc. Phys. Soc.* **81,** 1104.
13. MARTIENSSEN, W. and SPILLER, E. (1966). *Phys. Rev. Lett.* **16,** 531.
14. WOLF, R. P. and CROOKER, P. P. (1982). *Am. J. Phys.* **50,** 406.
15. STEEGER, P. F. and FERCHER, A. F. (1982). *Optica Acta* **29,** 1395.